Power System Technology
ISSN:1000-3673

Received: 06-04-2023 Revised: 15-05-2023 Accepted: 28-06-2023

Exact Solutions to MHD Flow Across a Vertical Channel Under Induced Magnetic Field and Chemical Reaction

Deepti[a], Jitendra Singh[b]

[a]Shivaji College, University of Delhi, India. Email: deepti@shivaji.du.ac.in

[b]Shivaji College, University of Delhi, India. Email: jitu.iitd@gmail.com

Abstract: This paper projects the impact of chemical reaction and induced magnetic field on steady fluid flow model through an infinite vertical channel. Also this model includes the source/sink of heat. The exact solutions are find out for this flow model which include equation of motion, heat equation and diffusion equation using dimensionless conversion method. Under this conversion, several fluid characterizing parameters have appeared and their impression on velocity, temperature, concentration, ICD and IMF profiles has been examined in terms of graphical presentation. Further, skin friction and mass transfer rate are evaluated numerically correspond to varying parameters and represented with the tables.

1. Introduction

Magneto hydrodynamics (MHD) has undergone a noticeable growth and diversification in both its scope and range of subject areas embraced by it. The exploration of hydro magnetic flow involving natural convection and the consideration of an applied magnetic field across various channels has garnered extensive attention due to its diverse applications in different scientific and engineering domains such as power generation in MHD generators, material processing, geophysical processes, heating and cooling systems. Numerous research endeavors have been undertaken to explore hydro magnetic natural convection across various channels w.r.t varying boundary and heating conditions. Such kind of exploration can be seen in the investigations of Morques et al [1], Chamkha [2], Makinde and Mohne [3], Hyat et al. [4], Singh and Singh [5], Aruna et al.[6] and Falade et al [7]. These studies have neglected the induced magnetic field effects for simplification purposes.

So in recent times, many academicians have studied the IMF impacts in their work due to their significance in many physical situations. Mazumdar et al. [8] studied the induced magnetic field effects by considering the Hall effects in the hydromagnetic flow of ECF under free and forced convection across parallel plate channel. Gosh [9] examined the impact of rotating channel on hydro magnetic viscous electrically conducting flow under induced magnetic field effects for steady and unsteady cases both. Singh et al [10] provided the numerical solutions to the flow analysis of ECF in vertical channel including the induced magnetic field effects and also he validates the solutions by comparing it with analytical solutions. Further Gosh [11] observed the noticeable impact of IMF on hydro magnetic free convection flow in the vicinity of an infinite vertical flat plate. Singh and Singh [12] discussed the impact of IMF on velocity profiles of steady flow driven by buoyancy forces in vertical annuli having same center with

Power System Technology
ISSN:1000-3673
Received: 06-04-2023 Revised: 15-05-2023 Accepted: 28-06-2023

steady heat flux. Jha and Isa [13] gave the numerical computation to the transient flow problem of hydro magnetic flow of ECF in vertical channel under symmetric heating wall conditions including the induced magnetic field effects. Also the researcher finds the good agreement of this solution with analytic solution in case of steady state flow. Sarveshanand and Singh [14] studied the IMF effect on steady 2-D hydro magnetic flow of ECF across the channel formed by two vertical parallel plates of porous nature and constant heat flux. Jha and Aina [15] analyzed the problem of IMF effect on taking velocity slip and temperature jump conditions on free convection hydro magnetic flow of electrically conducting flow in-between the walls of channel formed by electrically non conducting plates. Further Jha and Aina [16] discussed the previous problem by considering the mixed convection flow including pressure gradients in the flow analysis. Also, Jha and Aina [17] discussed the IMF effects on MHD mixed convection flow through a vertical microchannel formed by conducting and non-conducting infinite plates by taking velocity jump and temperature jump conditions at the walls. Furthermore, Jha and Aina[18] investigated the previous problem by replacing the vertical channel of parallel plates by annular micro channel. Mrinomy et al [19] studied analytically the IMF on unsteady MHD flow of electrically conducting fluid across the vertical channel in the presence of inclined magnetic field and plates are taken in motion opposite to each other. Recently, Dileep [20] has discussed the radiation and IMF effects on MHD flow across a vertical channel with Newtonian heating/cooling conditions at the walls. In these studies, mass transfer effects under chemical reaction has not been studied. As the integrated heat and mass transfer study have numerous applicability in various natural and engineering phenomenon such as salt transported by ocean currents, chemical catalytic processes, medicine diffusion in blood veins, chemical pollutants spreading in plants, migration of moisture in petroleum reservoirs etc. In such processes diffusion occurs due to some chemical reaction with fluid in contact and significantly affect the flow properties and enhance the product quality. In this work, we have pursued the exact solutions for heat and mass transfer flow model subjected to chemical change through the vertical channel by natural convection with heat source/ sink and IMF factor.

2. Mathematical Model of flow

The steady flow equations for MHD flow of ECF are given by.

Continuity Equation

$$\nabla . V = 0$$

Momentum Equation

$$\rho(V.\nabla)\mathrm{V} = -\nabla\mathrm{P} + \mu_e(\nabla^2 V) + J \times H + \rho g$$

Magnetic field equation

$$(\nabla^2 H) + \nabla \times (V \times H) = 0$$

Power System Technology
ISSN:1000-3673
Received: 06-04-2023 Revised: 15-05-2023 Accepted: 28-06-2023

Energy Equation

$$(V.\nabla)\mathrm{T} = \frac{\kappa}{\rho C_p}\nabla^2 T + \frac{Q_0}{\rho C_p}$$

Diffusion Equation

$$(V.\nabla)\mathrm{C} = \mathrm{D}\nabla^2 C - K_1 C$$

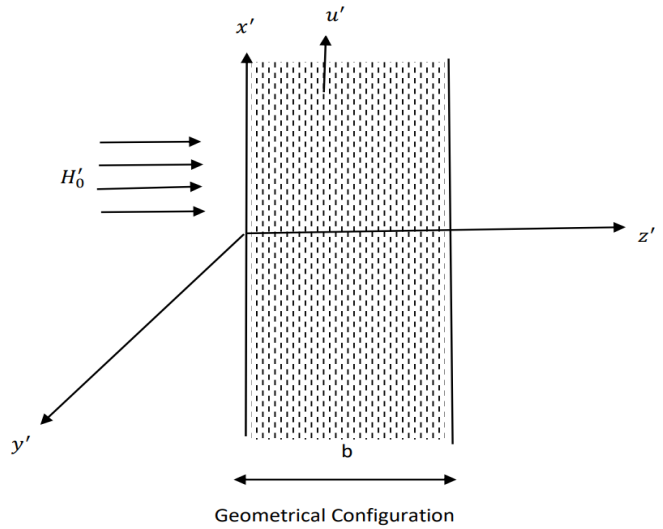

Geometrical Configuration

In this model, a vertical channel with non-conducting walls which are at 'b' distance apart is placed along x'- axis taken in vertical upward direction. A magnetic field of strength H_0' is employed parallel to z'- -axis which is taken perpendicular to the walls and y'-axis is taken normal to $x'z'$- plane. Further incompressible, viscous and electrically conducting fluid is projected through this channel with first order chemical reaction in the proximity of heat source/ sink. The temperature and concentration at the plate $z' = 0$ are assumed greater than the plate at $z' = b$. Also due to walls infinite extent in x' and y' directions, all dependent unknowns in fluid equations become the function of z'- only. Under the Boussinesq approximation, the existing model flow equations are:

$$\vartheta\frac{d^2u'}{dz'^2} + \frac{\mu_e H_0'}{\rho}\frac{dh'}{dz'} + g\beta(T' - T_b') + g\beta'(C' - C_b') = 0 \quad (1)$$

$$\frac{d^2h'}{dz'^2} + \sigma\mu_e H_0'\frac{du'}{dz'} = 0 \quad (2)$$

$$\frac{\kappa}{\rho C_p}\frac{d^2u'}{dz'^2} + \frac{Q_0}{\rho C_p}(T' - T_b') = 0 \quad (3)$$

$$\mathrm{D}\frac{d^2u'}{dz'^2} - k_1(C' - C_b') = 0 \quad (4)$$

Power System Technology
ISSN:1000-3673
Received: 06-04-2023 Revised: 15-05-2023 Accepted: 28-06-2023

With boundary conditions as

$$u' = 0,\ h' = 0,\quad T' = T'_b + (T'_0 - T'_b),\qquad C' = C'_b + (C'_0 - C'_b)\qquad at\ z' = 0$$

$$u' = 0,\ h' = 0,\quad T' = T'_b,\qquad C' = C'_b\qquad at\ z' = b \tag{5}$$

To convert the governing flow equations into non-dimension form, the following parameters and variables have been taken

$$v = \frac{u'}{U}, Z = \frac{z'}{b}, B = \frac{h'}{\sigma\mu_e H'_0 U b}, \theta = \frac{T'-T'_b}{T'_0-T'_b}, C = \frac{C'-C'_b}{C'_0-C'_b}, \mathrm{Gr} = \frac{g\beta(T'_0-T'_b)b^2}{\nu U},\ \mathrm{Gm} = \frac{g\beta'(C'_0-C'_b)b^2}{\nu U},$$

$$Ha = \mu_e H'_0 b\sqrt{\frac{\sigma}{\mu}}, S = -\frac{Q_0\, b^2}{\kappa}, \lambda = \frac{k_1 b^2}{D}$$

Above non dimensional quantities converts the equations (1) - (5) as

$$\frac{d^2v}{dz^2} + Ha^2\frac{dB}{dz} + Gr\,\theta + GmC = 0 \tag{6}$$

$$\frac{d^2B}{dz^2} + \frac{dv}{dz} = 0 \tag{7}$$

$$\frac{d^2\theta}{dz^2} - S\,\theta = 0 \tag{8}$$

$$\frac{d^2C}{dz^2} - \lambda\, C = 0 \tag{9}$$

$$v = 0,\ B = 0,\ \theta = 1,\ C = 1\qquad at\ z = 0$$

$$v = 0,\ B = 0,\ \theta = 0,\ C = 0\qquad at\ z = 1 \tag{10}$$

3. Analytical Solution method

Using simultaneous ODE system, the analytical solutions for the equations (6)-(9) subjected to boundary conditions (10) has been given by

$$v = -H\,d_5\exp(H\,z) + H\,d_6\exp(-H\,z) - \frac{Gr}{(S-H^2)}\left(d_3\exp\left(\sqrt{S}z\right) + d_4\exp\left(-\sqrt{S}z\right)\right) - \frac{Gm}{(\lambda-H^2)}\left(d_1\exp\left(\sqrt{\lambda}z\right) + d_2\exp\left(-\sqrt{\lambda}z\right)\right) + d_8 \tag{10}$$

Power System Technology
ISSN:1000-3673
Received: 06-04-2023 Revised: 15-05-2023 Accepted: 28-06-2023

$$B = d_7 + d_5 \exp(H\,z) + d_6 \exp(-H\,z) + \frac{Gr}{\sqrt{S}\,(S-H^2)}\left(d_3 \exp\left(\sqrt{S}z\right) - d_4 \exp\left(-\sqrt{S}z\right)\right) + \frac{Gm}{\sqrt{\lambda}\,(\lambda-H^2)}\left(d_1 \exp\left(\sqrt{\lambda}z\right) - d_2 \exp\left(-\sqrt{\lambda}z\right)\right) \quad (11)$$

$$\theta = d_3 \exp\left(\sqrt{S}z\right) + d_4 \exp\left(-\sqrt{S}z\right) \quad (12)$$

$$C = d_1 \exp\left(\sqrt{\lambda}z\right) + d_2 \exp\left(-\sqrt{\lambda}z\right) \quad (13)$$

The other variables ICD (J) and skin friction (τ) are given by

$$J = -\frac{dB}{dz} = -d_5 H \exp(H\,z) + d_6 H \exp(-H\,z) - \frac{Gr}{\sqrt{S}\,(S-H^2)}\left(d_3\sqrt{S} \exp\left(\sqrt{S}z\right) + d_4\sqrt{S}\exp\left(-\sqrt{S}z\right)\right) - \frac{Gm}{\sqrt{\lambda}\,(\lambda-H^2)}\left(d_1\sqrt{\lambda} \exp\left(\sqrt{\lambda}z\right) + d_2\sqrt{\lambda} \exp\left(-\sqrt{\lambda}z\right)\right) \quad (14)$$

$$(\tau)_{z=0} = \left(\frac{\partial \mathrm{v}}{\partial \mathrm{z}}\right)_{z=0} = -H^2\,d_5 - H^2\,d_6 - \frac{Gr\sqrt{S}}{(S-H^2)}(d_3 - d_4) - \frac{Gm\sqrt{\lambda}}{(\lambda-H^2)}(d_1 - d_2) \quad (15)$$

$$(\tau)_{z=1} = -\left(\frac{\partial \mathrm{v}}{\partial \mathrm{z}}\right)_{z=1} = H^2\,d_5 \exp(H\,) + H^2\,d_6 \exp(-H\,) + \frac{Gr}{(S-H^2)}\left(d_3\sqrt{S} \exp\left(\sqrt{S}\right) - d_4\sqrt{S} \exp\left(-\sqrt{S}\right)\right) + \frac{Gm}{(\lambda-H^2)}\left(d_1\sqrt{\lambda} \exp\left(\sqrt{\lambda}\right) - d_2\sqrt{\lambda} \exp\left(-\sqrt{\lambda}\right)\right) \quad (16)$$

The rate of mass transfer through both plates represented by Sherwood number is defined as

$$(Sh)_{z=0} = -\left(\frac{dC}{dz}\right)_{z=0} = -d_1\sqrt{\lambda} + d_2\sqrt{\lambda} \quad (17)$$

$$(Sh)_{z=1} = -\left(\frac{dC}{dz}\right)_{z=1} = -d_1\sqrt{\lambda} \exp\left(\sqrt{\lambda}\right) + d_2\sqrt{\lambda} \exp\left(-\sqrt{\lambda}\right) \quad (18)$$

4. Graphical Interpretation of Results

In this part, the solutions obtained for v, θ, C and B are displayed through graphs to visualize the impression of flow parameters- Ha, Gr Gm, S and λ. Also, skin friction at the channel plates are numerically evaluated and put in the table form for the clear observance.

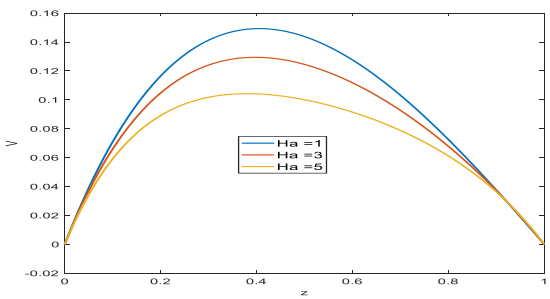

Fig 1. Velocity correspond to varying Ha

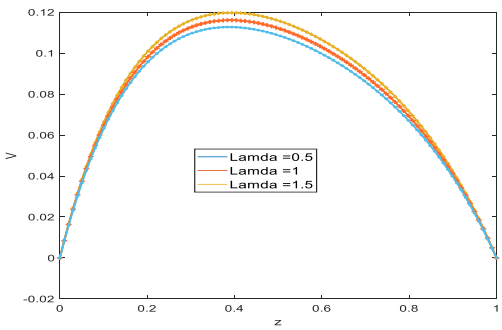

Fig 2. Velocity correspond to varying λ

Power System Technology
ISSN:1000-3673

Received: 06-04-2023 Revised: 15-05-2023 Accepted: 28-06-2023

The velocity variations w.r.t to varying parameters can be visualized via the Figures 1-5. A gradual fall in the velocity graphs (Figure 1) has been observed with the increment in Ha values which reflects that in the existence IMF and heat source, electromagnetic forces become more dominant and slows down the flow. Figures 3-5 demonstrates the variation of velocity corresponding to lambda, Gr and Gm values. They show that the velocity graphs are risen with the hike in these values. This signifies that chemical reaction and buoyancy forces dominates the viscous forces which accelerate the fluid flow. The behavior of IMF profiles in the channel can be visualized through the figures 6-10. This behavior is different in the whole region of the channel. It is noted that the increment in lambda and Ha values lower the graphs near the left plate but behave adversely close to right plate. It can be interpreted that electromagnetic force and chemical reaction have strong impact in the left part to the centre of channel and this impact is reversed in other part. However the overall behavior of IMF profile is that it firstly increases till the centre of channel and starts gradually decreasing and near to right plate it again rise up to 0

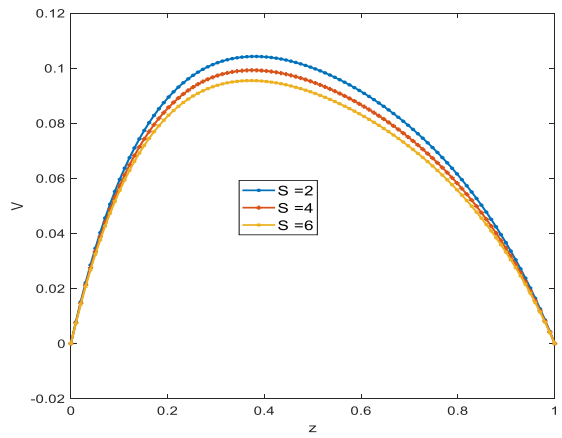

Fig 3. Velocity correspond to varying S

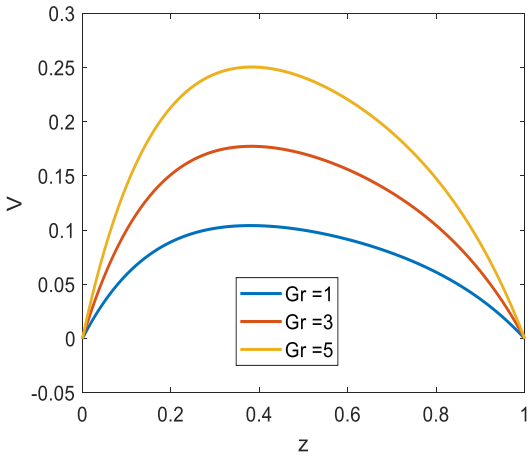

Fig 4. Velocity correspond to varying Gr

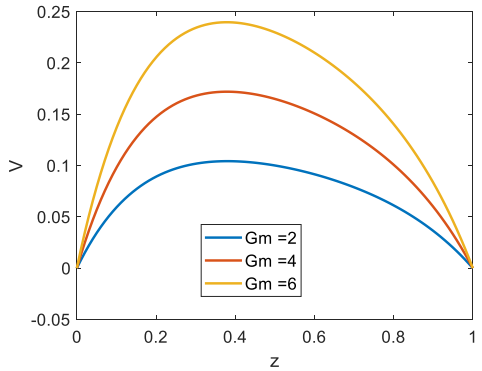

Fig 5. Velocity correspond to varying Gm

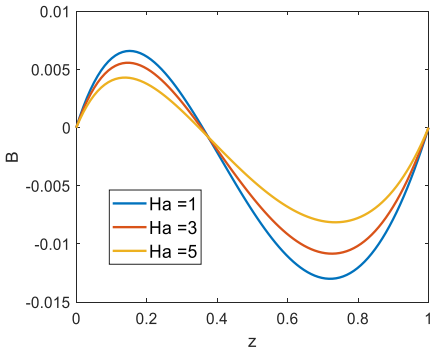

Fig. 6 Velocity correspond to varying Ha

Power System Technology
ISSN:1000-3673

Received: 06-04-2023 Revised: 15-05-2023 Accepted: 28-06-2023

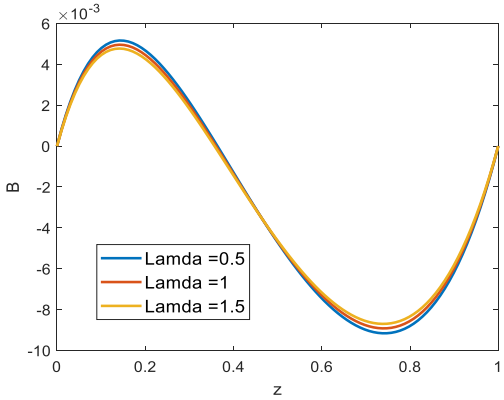

Fig 7. IMF correspond to varying λ

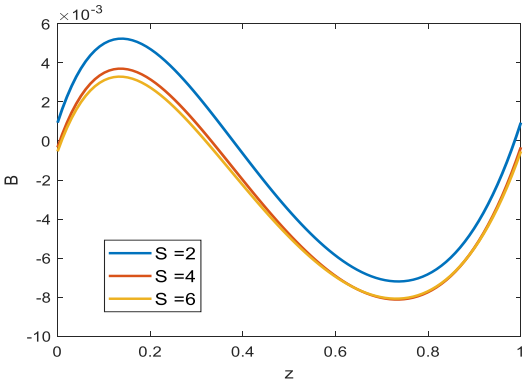

Fig. 8 IMF correspond to varying S

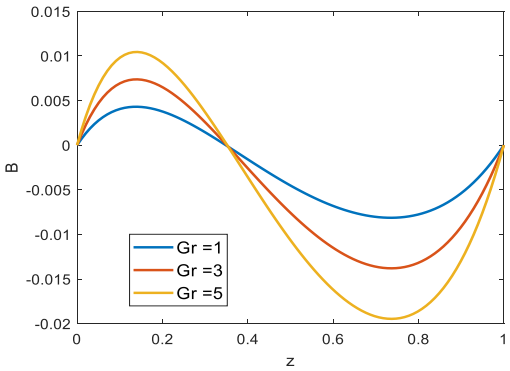

Fig 9. IMF correspond to varying Gr

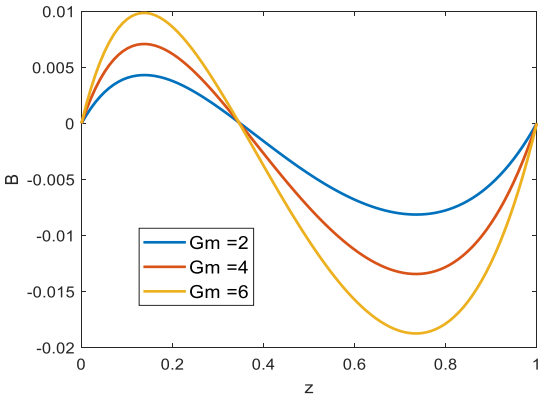

Fig 10. IMF correspond to varying Gm

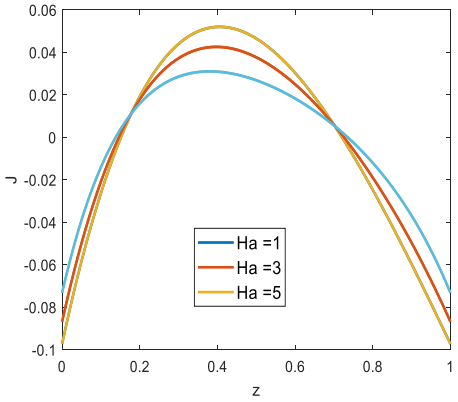

Fig 11. ICD correspond to varying Ha

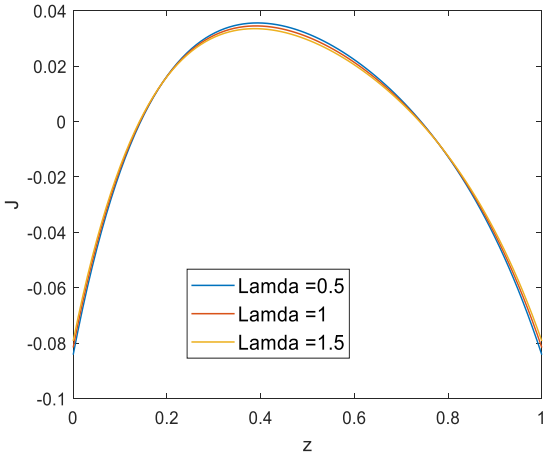

Fig 12. ICD correspond to varying λ

Power System Technology
ISSN:1000-3673
Received: 06-04-2023 Revised: 15-05-2023 Accepted: 28-06-2023

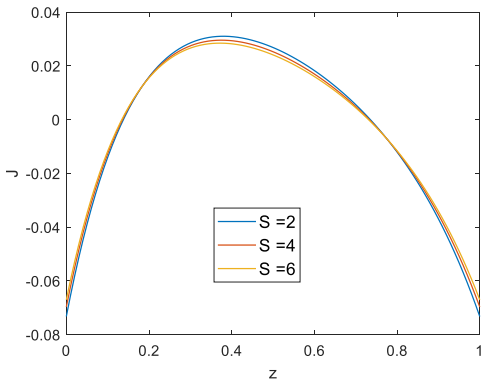

Fig 13. ICD correspond to varying S

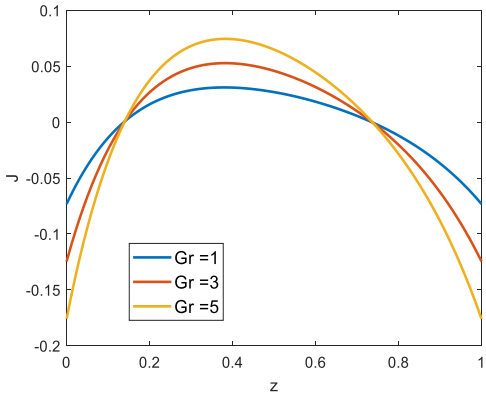

Fig 14. ICD correspond to varying Gr

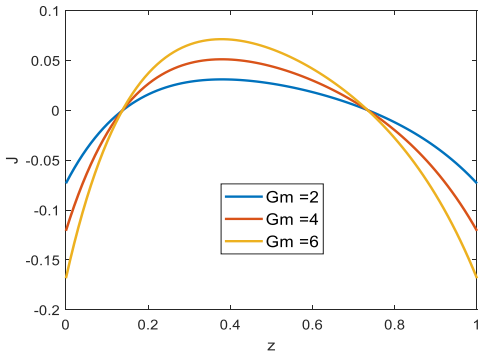

Fig 15. ICD correspond to varying Gm

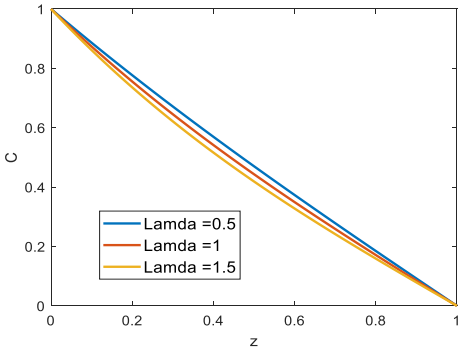

Fig 16. ICD correspond to varying λ

The fluctuations in ICD graphs are laid out in the Figures 11-15. A fascinating behavior has been observed in ICD graphs with the fluctuations in Ha, Gr and Gm values. The graphs (Figures 11, 14 and 15) show decreasing behavior close to left plate and suddenly increases around the middle of channel and then decline as approaching to right plate of the channel. This reflects that the viscous forces become weak in the region of center of channel which imparts in accelerating the flow. Figures 12-13 showcase the parabolic nature of ICD profiles w.r.t change in the values of gamma and S. The ICD profiles has been seen compressed with the increment in S and Gamma values which interprets that the mass diffusion and energy redistribution slower down the induced current density. Figure 16 reveals the decrease in concentration with the increment in gamma values which embarks that the chemical reaction in the channel slower down the mass diffusion process. The drag at the plates of the channel are calculated w.r.t varying parameters Ha, λ and Gm which are laid out in Table 1 and 2. The increment in Ha values imparts the increase in drag at left plate but reduces the drag at the right plate. This signifies that the Lorentz forces are more effective at the left plate as compared to right one. The drag the both plates shows decline pattern with increment in chemical reaction parameter values

Power System Technology
ISSN:1000-3673
Received: 06-04-2023 Revised: 15-05-2023 Accepted: 28-06-2023

Table 1. Skin friction with varying parameter values at the plate z = 0

Ha	τ_0	λ	τ_0	Gm	τ_0
1	0.8548	0.5	0.8769	2	0.7965
3	0.8295	1	0.8581	4	1.3180
5	0.7965	3	0.7965	6	1.8396

Table 2. Skin friction with varying parameter values at the plate z = 1

Ha	τ_1	λ	τ_1	Gm	τ_1
1	0.3833	0.5	0.5139	2	0.4416
3	0.4086	1	0.4967	4	0.7276
5	0.4416	3	0.4416	6	1.0136

Further the rise in Gm values predicts the improvement in skin friction values at both plates. The rate of mass transfer across both the plates are set out in Table 3. The mass transfer rate designated by Sherwood number is accelerated at the left plate with the increase in λ values but shows decelerated close to right plate of channel

Table 3. Sherwood number with varying λ at plates z = 0 and z = 1

λ	Sh_0	Sh_1
0.5	1.1614	-2.3554
1	1.3130	-3.5692
3	1.8440	-10.4226

Conclusion

The outputs of the current work are culminated as:

- Induced magnetic field significantly lower down the velocities throughout the channel region and chemical reaction accelerates this behavior.
- IMF profiles exhibits the falling off nature to the left of middle of the channel and risen up to the right of middle of the channel due to IMF and chemical reaction.
- IMF causes the reduction in drag at the left plate but promotes the drag at the right plate. However the chemical reaction turn down the drag at the both plates.
- The chemical reaction in the flow enhanced the mass transfer rate at the left plate whereas it is weaken close to the right plate

So here, we inference that the flows infused with IMF and chemical reaction are significantly influenced which can contribute towards the betterment of many electrical devices, medical equipments and industrial processes.

Power System Technology
ISSN:1000-3673
Received: 06-04-2023 Revised: 15-05-2023 Accepted: 28-06-2023

The quantities $d_i, i = 1,2, \ldots 8$ are given in the appendix

Appendix

$$d_1 = \frac{-e^{-2\sqrt{\lambda}}}{1-e^{-2\sqrt{\lambda}}}, \quad d_2 = \frac{1}{1-e^{-2\sqrt{\lambda}}}, \qquad d_3 = \frac{-e^{-2\sqrt{S}}}{1-e^{-2\sqrt{S}}}, \quad d_4 = \frac{1}{1-e^{-2\sqrt{S}}},$$

$$d_5 = \frac{-1}{2(1-e^{H})}\left(\frac{Gr}{(S-H^2)}\left(d_3\left(1-e^{\sqrt{S}}\right)\left(\frac{1}{\sqrt{S}}+\frac{1}{H}\right)-d_4(1-e^{-\sqrt{S}})\left(\frac{1}{\sqrt{S}}-\frac{1}{H}\right)\right)\right.$$
$$\left.+\frac{Gm}{(\lambda-H^2)}\left(d_1\left(1-e^{\sqrt{\lambda}}\right)\left(\frac{1}{\sqrt{\lambda}}+\frac{1}{H}\right)-d_2(1-e^{-\sqrt{\lambda}})\left(\frac{1}{\sqrt{\lambda}}-\frac{1}{H}\right)\right)\right)$$

$$d_6 = \frac{-1}{2(1-e^{-H})}\left(\frac{Gr}{(S-H^2)}\left(d_3\left(1-e^{\sqrt{S}}\right)\left(\frac{1}{\sqrt{S}}-\frac{1}{H}\right)-d_4(1-e^{-\sqrt{S}})\left(\frac{1}{\sqrt{S}}+\frac{1}{H}\right)\right)\right.$$
$$\left.+\frac{Gm}{(\lambda-H^2)}\left(d_1\left(1-e^{\sqrt{\lambda}}\right)\left(\frac{1}{\sqrt{\lambda}}-\frac{1}{H}\right)-d_2(1-e^{-\sqrt{\lambda}})\left(\frac{1}{\sqrt{\lambda}}+\frac{1}{H}\right)\right)\right)$$

$$d_7 = -\frac{Gr(d_3-d_4)}{\sqrt{S}\,(S-H^2)}-\frac{Gm\,(d_1-d_2)}{\sqrt{\lambda}\,(\lambda-H^2)}-d_6-d_5$$

$$d_8 = \frac{Gr(d_3+d_4)}{(S-H^2)}+\frac{Gm\,(d_1+d_2)}{(\lambda-H^2)}-H\,d_6+H\,d_5$$

Nomenclature

ν	Coefficient of Kinematic viscosity, m^2s^{-1}
β	Volumetric coefficient of thermal expansion, K^{-1}
β′	Volumetric coefficient of expansion of concentration, K^{-1}
μ	Coefficient of viscosity, $kgm^{-1}s^{-1}$
κ	Thermal conductivity, $Wm^{-1}K^{-1}$
ρ	Fluid density, kgm^{-3}
σ	Electrical conductivity, $\Omega^{-1}m^{-1}$

Power System Technology
ISSN:1000-3673
Received: 06-04-2023 Revised: 15-05-2023 Accepted: 28-06-2023

λ	Chemical reaction parameter
μ_e	Magnetic permeability
h	
B	Induced Magnetic Field
C'	Dimensional species concentration, Kgm^{-3}
C'_0	Free stream species concentration, Kgm^{-3}
C'_b	Species concentration at the wall, Kgm^{-3}
D	Chemical molecular diffusivity, m^2s^{-1}
ECF	Electrically Conducting Fluid
Q_0	Heat source/sink coefficient
Gm	Mass Grashof number
Gr	Thermal Grashof number
H_0	Strength of applied magnetic field, Wbm^{-2}
Ha	Hartmann number
ICD	Induced Current Density
S	Heat source/sink parameter
Sh	Sherwood number
θ	Dimensionless fluid temperature
T_0'	Temperature of the fluid and plates in reference state, K
T'	Dimensional fluid temperature,
T'_b	Fluid temperature at wall, K

Power System Technology
ISSN:1000-3673

Received: 06-04-2023 Revised: 15-05-2023 Accepted: 28-06-2023

IMF Induced Magnetic Field

Declaration

The authors affirms no financial or other conflicts of interest.

Bibliography

1. Morques, Jr. W., Kermer, G. M., and Shapiro, F. M., (2000), "The effect of slip condition on unsteady MHD oscillatory flow of viscous fluid in a planner channel", Rom. J. Phys., **52**, pp. 85–91.
2. Chamkha A. J., (2002), "On laminar mixed convection flows in a vertical channel with symmetric and asymmetric wall heating conditions", Int. J. Heat Mass Transfer, **45**, pp. 2509–2525.
3. Makinde, O. D., and Mhone, P. Y., (2005), "Heat transfer to MHD oscillatory flow in a channel filled with porous medium", Rom. J. Phys., **50**, pp. 931–938.
4. Hayat, T., Ahmed, N., Sajid, M., And Asghar, S., (2007), "On the MHD flow of second grade fluid in a porous channel", Compt. Math Appl., **54**, pp. 407–414.
5. Singh, R. K., Singh, A. K.: Hydromagnetic mixed convection between two vertical walls. Journal of Energy, Heat and Mass Transfer 31, 111–123 (2009)
6. Aruna, G., Rama, B., Reddy, B., Varma, S. V. K., and Iyengar N. CH. S. N., (2011), "A numerical study on developed MHD Laminar mixed convection in vertical channels", J. Comp.& Math. Sci., **2**, pp. 336–351.
7. Falade J.A. , Ukaegbu Joel C. , Egere A.C., Adesanya Samuel O., (2017), MHD oscillatory flow through a porous channel saturated with porous medium, Alexandria Engineering Journal 56, 147–152.
8. Mazumdar, B. S., Gupta, A. S., and Datta, N., (1976), "Hall effects on combined free and forced hydromagnetic flow through a channel", Int. J. Engg. Sci., **14**, pp. 285–292
9. Gosh, S. K., (1991), "A note on steady and unsteady hydro magnetic flow in a rotating channel in the presence of inclined magnetic field", Int. J. of Engg. Sci., **29**, pp.1013-1016.
10. R.K. Singh, A.K. Singh, N.C. Sachetiand P. Chandran (2010). On hydromagnetic free convection in the presence of induced magnetic field, Heat Mass Transfer, 46, 523-529.
11. S.K.Ghosh, O.A. Beg and J. Zueco (2010). Hydromagnetic free convection flow with induced magnetic field effects, Meccanica, 14, 175-185.
12. R.K. Singh, A.K. Singh, Effect of induced magnetic field on natural convection in vertical concentric annuli, Acta Mech. Sin. 28 (2012) 3
13. B.K. Jha, I. Sani, Computational treatment of MHD of transient natural convection flow in a vertical channel due to symmetric heating in presence of induced magnetic field, J. Phys. Soc. Japan 82 (2013) 084401.

Power System Technology
ISSN:1000-3673

Received: 06-04-2023 Revised: 15-05-2023 Accepted: 28-06-2023

14. Sarveshanand, A.K. Singh, Magnetohydrodynamic free convection between vertical parallel porous plates in the presence of induced magnetic field, Springer Plus 4 (2015) 333.
15. B.K. Jha, B. Aina (2016), Role of induced magnetic field on MHD natural convection flow in vertical microchannel formed by two electrically non-conducting infinite vertical parallel plates, Alexandria Engineering Journal 55, 2087–2097
16. B.K. Jha, B. Aina (2017), Effect of induced magnetic field on mhd mixed convection flow in vertical microchannel, Int. J. Appl. Mech. Eng. 22 567-582.
17. B.K Jha and B. Aina (2017), Impact of Induced Magnetic Field on Magnetohydrodynamics Mixed Convection Flow in Vertical Microchannel Formed by Non-Conducting and Conducting Infinite Vertical Parallel Plates, Journal of Nano fluids,6960-970.
18. B.K Jha and B. Aina(2018), Impact of induced magnetic field on magnetohydrodynamic (MHD) natural convection flow in a vertical annular microchannel in the presence of radial magnetic field, Propulsion and Power Research, 7(2):171–181
19. M. Goswami, K. G. Singha, A. Goswami, P.N.DEKA(2018), A Study of Unsteady MHD Vertical Flow of an Incompressible, Viscous, Electrically conducting Fluid bounded by Two Non-Conducting Plates in Presence of a Uniform inclined Magnetic Field, Proceedings of the World Congress on Engineering, 1 , London, U.K.
20. D. Kumar (2021) , Radiation effect on magnetohydrodynamic flow with induced magnetic field and Newtonian heating/cooling: an analytic approach, Propulsion and Power Research 10(3), 310-313